

000 001 002 003 004 005 006 007 008 009 010 011 012 013 014 015 016 017 018 019 020 021 022 023 024 025 026 027 028 029 030 031 032 033 034 035 036 037 038 039 040 041 042 043 044 045 046 047 048 049 050 051 052 053 POLICY IMPROVEMENT WITH STYLE-SPECIFIC DEMONSTRATIONS

Anonymous authors

Paper under double-blind review

ABSTRACT

Proficient game agents with diverse play styles enrich the gaming experience and enhance the replay value of games. However, recent advancements in game AI based on reinforcement learning have predominantly focused on improving proficiency, whereas methods based on evolution algorithms generate agents with diverse play styles but exhibit subpar performance compared to RL methods. To address this gap, this paper proposes Mixed Proximal Policy Optimization (MPPO), a method designed to improve the proficiency of existing suboptimal agents while retaining their distinct styles. MPPO unifies loss objectives for both online and offline samples and introduces an implicit constraint to approximate demonstrator policies by adjusting the empirical distribution of samples. Empirical results across environments of varying scales demonstrate that MPPO achieves proficiency levels comparable to, or even superior to, pure online algorithms while preserving demonstrators' play styles. This work presents an effective approach for generating highly proficient and diverse game agents, ultimately contributing to more engaging gameplay experiences.

1 INTRODUCTION

Games benefit from having bots with varied proficiency and diverse play styles. Bots with different levels of proficiency accommodate a wider range of players, providing smoother gaming experiences (Climent et al., 2024; Romero-Mendez et al., 2023). In games featuring competition and cooperation, distinct agent styles provide value both as diversified opponents (Barros et al., 2023) and as adaptive partners for players with varied strategic preferences (Sweller, 1994; Chen, 2017). This is particularly evident in contemporary games that incorporate heterogeneous agents. From aggressive melee assassins to defensive support mages, characters in MOBA titles (Dota 2, League of Legends) and hero shooters (Valorant, Overwatch) possess distinct gameplay mechanics, and corresponding AI agents must replicate these stylistic nuances to provide immersive player experiences (Gao et al., 2023).

Advancement and application of Reinforcement Learning (RL) in game AI elevate agents' proficiency across various games. In traditional games, AlphaZero defeats top humans in chess, Shogi, and Go (Silver et al., 2017); PerfectDou (Yang et al., 2024) outperforms other AIs in DouDiZhu; AlphaHoldem (Zhao et al., 2022) beats human professionals in Texas Hold'em Poker. In computer games, AlphaStar (Vinyals et al., 2019) reaches grandmaster level in StarCraft II, OpenAI Five (Berner et al., 2019) defeats the Dota 2 world champion team, and JueWu (Ye et al., 2020) beats top esport players in The Honor of Kings. However, these methods prioritize reward maximization, and agents' play styles are not within their considerations.

The pursuit of diverse game-playing agents has attracted growing interest. While Quality-Diversity (QD) optimization (Lehman & Stanley, 2011) methods have been applied to generate varied behaviors (Canaan et al., 2019; Perez-Liebana et al., 2020), they often rely on predefined behavior descriptors and archive structures, which can limit their scalability and performance in complex domains like image-based games (Fuks et al., 2019; Chen et al., 2019; Badia et al., 2020). Meanwhile, within RL, population-based algorithms have emerged as a promising paradigm for fostering strategic diversity. These methods induce behavioral heterogeneity by optimizing agents towards divergent objectives, such as employing distinct risk preferences (Jiang et al., 2023), randomizing

054 reward functions (Tang et al., 2021), or directly maximizing a diversity metric (Parker-Holder et al.,
 055 2020) like the determinant of the population’s behavioral embedding matrix.

056
 057 While effective for discovering diverse behaviors, these population-based methods come at the sig-
 058 nificant computational cost of maintaining a large agent cohort and offer limited control over steering
 059 strategies toward a predefined style.

060 We therefore introduce a method that complements the population-based paradigm by efficiently
 061 “polishing” individual agents. Our approach tackles the distinct problem of *single-agent policy*
 062 *optimization with style preservation*: given suboptimal, stylized agents, we enhance their proficiency
 063 while preserving their play styles. To this end, we propose **Mixed Proximal Policy Optimization**
 064 (MPPO), a Learning from Demonstration (LfD) algorithm that leverages existing demonstrators to
 065 achieve this goal. Specifically, we employ two types of actors: on-policy actors improve policies and
 066 generalize learned behaviors to unseen states, while LfD actors imitate the demonstrators’ policies.
 067 Samples generated by these actors are processed and trained using unified loss objectives. Through
 068 theoretical analysis, we prove that our method can monotonically improve the policy while satisfying
 069 implicit behavior cloning constraints. We test MPPO in three environments of varying complexity:
 070 Blackjack, Maze Navigation, and Mahjong. Empirical results demonstrate that MPPO is comparable
 071 or superior to baseline methods, achieving meaningful improvements in agent proficiency while
 072 retaining the unique characteristics of the original play styles. Notably, starting from suboptimal
 073 demonstrations, one of our Mahjong agents surpasses the top-ranked bot on Botzone’s Elo ranking
 074 list (Zhou et al., 2018). The following are the key contributions of this paper:

- 075 • This paper proposes MPPO, a method that leverages data from suboptimal demonstrators to
 076 enhance policy proficiency while maintaining a relatively small distance from the demon-
 077 strators’ policies.
- 078 • Theoretically, we demonstrate that our loss objectives are capable of monotonically im-
 079 proving the policy while guiding the student policy to imitate the demonstrator’s.
- 080 • Enhancements to offline dataset collection and replay mechanisms enable the straightfor-
 081 ward application of Monte Carlo-based advantage estimation, while reducing the storage
 082 footprint by at least 98% in our test scenarios.
- 083 • We present a suite of environments of varying scales as a benchmark to test agents’ play
 084 style diversity and proficiency, with each environment accompanied by multiple stylized
 085 bots. In addition, we introduce a metric, D_{policy} , to quantify differences in play styles.

086 2 RELATED WORKS

087 Learning from Demonstration (LfD) is a broad research area that focuses on improving agents’
 088 learning efficiency by leveraging demonstration data to reduce the cost of agents’ blind trial-and-
 089 error in environments. Based on whether methods integrate RL, LfD methods can be categorized
 090 into two categories: pure Imitation Learning (IL) (Zare et al., 2024), which learns policies solely
 091 through imitating experts’ behaviors, and RL combined with demonstration learning, which utilizes
 092 demonstration data to accelerate the RL process.

093 Generative Adversarial Imitation Learning (GAIL) (Ho & Ermon, 2016) is a prominent IL method
 094 that considers IL problems as distribution matching, and it integrates adversarial training tech-
 095 niques (Goodfellow et al., 2014) to assign rewards for actions. Although this architecture solves
 096 challenges from sparse reward, students can hardly surpass demonstrator policies. POfD (Kang
 097 et al., 2018) and SAIL (Zhu et al., 2020) are GAN-based methods that build upon GAIL to address
 098 its limitations. However, these GAN-based methods suffer from inherent limitations of adversarial
 099 training, such as training instability and limited scalability in high dimensions (Brown et al., 2019).

100 Combining demonstration learning with reinforcement learning (RL) is appropriately termed Rein-
 101 force learning with Expert Demonstrations (RLED) (Piot et al., 2014). The core difference
 102 between RLED and IL is that the rewards are generated by the environment in RLED. The primary
 103 goal of methods (Chemali & Lazaric, 2015; Wagenmaker & Pacchiano, 2023; Hou et al., 2024) in
 104 this paradigm is to accelerate training or enhance performance using expert demonstrations, which
 105 aligns with our research focus. Additionally, our approach aims to **preserve the demonstrators’**
 106 **behavioral styles**.

108 Under the paradigm of RLED, existing approaches diverge in how they integrate offline data. Some
 109 methods employ a sequential strategy, pre-training on demonstrator data before fine-tuning with
 110 online interactions (Nair et al., 2021; Nakamoto et al., 2024), while others leverage offline and
 111 online data concurrently throughout training (Hester et al., 2017; Ball et al., 2023).

112 Since our primary objective is to achieve policy improvement while preserving the play style of
 113 the original demonstrators, we adopt the latter approach, which allows continuous guidance from
 114 demonstration data during policy optimization. Within this concurrent learning setting, a number
 115 of methods have been tailored to specific action space structures. For instance, DDPGfD (Vecerík
 116 et al., 2017) and RLPD (Ball et al., 2023) are designed for continuous control domains, whereas
 117 DQfD (Hester et al., 2017) represents a leading approach tailored to discrete action spaces, a com-
 118 mon setting in game environments that motivates our approaches.

119 DQfD integrates deep Q-learning (Mnih et al., 2013) with demonstration data by combining multi-
 120 step temporal difference (TD) and supervised losses, aiming to address state distribution bias and
 121 accelerate the convergence of the learning process. While our method aligns with DQfD in terms of
 122 application settings, there are key distinctions beyond the differences in their backbone algorithms.
 123 Specifically, DQfD employs explicit supervised losses to guide student policies; instead, we utilize
 124 implicit soft constraints to guide student policies through demonstration data filtering—this is rooted
 125 in our prior awareness that demonstrations may be suboptimal. Furthermore, we incorporate multi-
 126 step TD into Generalized Advantage Estimation (GAE) (Schulman et al., 2015), which significantly
 127 simplifies the algorithm’s architecture.

3 PRELIMINARIES

131 We formulate game environments as standard Markov Decision Processes (MDP) $\mathcal{M} =$
 132 $\langle \mathcal{S}, \mathcal{A}, R, \mathcal{P}, \gamma, \rho_0 \rangle$, where \mathcal{S} and \mathcal{A} are the observable state space and the action space, respec-
 133 tively, $R(s, a)$ represents the reward function, and $\gamma \in (0, 1)$ is the discount factor. ρ_0 is the initial
 134 state distribution. Policy $\pi(a_t|s_t)$ is defined as the distribution of actions conditioned on states at
 135 step t , where $s_t \in \mathcal{S}$ and $a_t \in \mathcal{A}$. $\mathcal{P}(s'|s, a)$ is the transition distribution of taking action a at
 136 observable state s . Both randomness from environment dynamics and randomness due to unob-
 137 servable state information are attributed to \mathcal{P} in the formulation. The trajectory $\tau = \{s_t, a_t\}_{t=0}^T$.
 138 The performance measure of policy is defined as $J(\pi) = \mathbb{E}_\pi \sum_{t=0}^T \gamma^t R(s_t, a_t)$. Then, the value
 139 function, state-value function, and the advantage function can be defined as $V_\pi(s) = J(\pi|s_0 = s)$,
 140 $Q_\pi(s, a) = J(\pi|s_0 = s, a_0 = a)$, and $A_\pi(s, a) = Q_\pi(s, a) - V_\pi(s)$, respectively.

141 **Theorem 1.** (Kakade & Langford, 2002) Let the discounted unnormalized visitation frequencies
 142 as $\rho_\pi(s) = \sum_{t=0}^T \gamma^t P(s_t = s|\pi)$, and $P(s_t = s|\pi)$ represents the probability of the t -th state equals
 143 to s in trajectories generated by policy π . For any two policies π and π' , the performance difference
 144 $J_\Delta(\pi', \pi) \triangleq J(\pi') - J(\pi)$ can be measured by:

$$J_\Delta(\pi', \pi) = \mathbb{E}_{s \sim \rho_{\pi'}(\cdot), a \sim \pi'(\cdot|s)} [A_\pi(s, a)]. \quad (1)$$

145 This theorem implies that improving policy from π to π' can be achieved by maximizing equation 1.
 146 From this theorem, Trust Region Policy Optimization (TRPO) (Schulman et al., 2017a) and Behav-
 147 ior Proximal Policy Optimization (BPPO) (Zhuang et al., 2023) are derived, which can guarantee
 148 the monotonic performance improvement for online and offline settings, respectively.

149 **Metric for Play Style Distance** To quantify the similarity between play styles, metrics are defined
 150 based on action distributions. Lin et al. (2024) used the 2-Wasserstein distance (W_2) (Vaserstein,
 151 1969) to measure the distance between play styles; however, W_2 is computationally expensive as a
 152 metric. More critically, its value depends on an arbitrary embedding of actions into a metric space
 153 to define pairwise distances. This makes results inconsistent and difficult to interpret, as different
 154 embeddings yield different distances for the same policies. Thus, we use total variational divergence,
 155 denoted as D_{policy} , to overcome W_2 ’s drawbacks and measure play style distances. Defined in
 156 equation 2, it quantifies action-level play style discrepancies.

$$D_{policy} = \mathbb{E}_{s \in S} \frac{1}{2} \sum_{a \in A} |\pi_1(a|s) - \pi_2(a|s)| \quad (2)$$

162

4 PROPOSED ALGORITHM

163

164 Our algorithm integrates data from both online environmental interactions and offline demonstration
165 datasets. We therefore term it **Mixed Proximal Policy Optimization** (MPPO).
166

167 In this section, we establish two fundamental theoretical properties of MPPO: 1) the policy improves
168 monotonically, and 2) the policy remains proximal to the demonstration policy throughout the learning
169 process. Subsequently, we provide the pseudocode and implementation details of MPPO.

170 We denote collections of demonstration trajectories as $D = \{\tau_1, \tau_2, \dots, \tau_N\}$ and the policy at some
171 point during the learning process as π_k . Our approach to policy improvement builds upon Theorem
172 1. However, directly optimizing equation 1 is intractable due to its dependence on the unknown
173 state distribution $\rho_{\pi'_k}(s)$ of the new policy. Standard online RL methods, such as TRPO, address
174 this by approximating $\rho_{\pi'_k}(s)$ with $\rho_{\pi_k}(s)$, the state distribution of the current policy π_k , thereby
175 guaranteeing monotonic improvement under on-policy data.

176 In our setting, which incorporates off-policy demonstration data, we propose a mixed state dis-
177 tribution. We sample a fraction β of state-action tuples from the demonstration dataset D , and
178 the remainder $1 - \beta$ from the current policy π_k . This leads to the empirical state distribution
179 $\rho_{mix}(s) = \beta\rho_D(s) + (1 - \beta)\rho_{\pi_k}(s)$, where $\rho_D(s)$ is the state visitation distribution in the demon-
180 stration data. Substituting this mixed distribution into equation 1 yields the following surrogate
181 objective:

182
$$\hat{J}_\Delta(\pi, \pi_k) = \mathbb{E}_{s \sim \beta\rho_D(\cdot) + (1 - \beta)\rho_{\pi_k}(\cdot), a \sim \pi(\cdot|s)} [A_{\pi_k}(s, a)]$$
183
184
$$= \beta \mathbb{E}_{s \sim \rho_D(\cdot), a \sim \pi(\cdot|s)} A_{\pi_k}(s, a) + (1 - \beta) \mathbb{E}_{s \sim \rho_{\pi_k}(\cdot), a \sim \pi(\cdot|s)} A_{\pi_k}(s, a) \quad (3)$$
185

186 The monotonic improvement guarantee for the second term in equation 3, which handles on-policy
187 data, is well-established by TRPO. For the first term, which utilizes off-policy demonstration data,
188 recent work on BPPO provides analogous theoretical guarantees, ensuring improvement under static
189 dataset constraints. We leverage these prior theoretical results. Since our objective is a linear com-
190 bination of the objectives from TRPO and BPPO, the monotonic improvement property is preserved
191 for the combined objective \hat{J}_Δ .

192 For practical implementation and stability, we adopt the clipped surrogate objective from Proximal
193 Policy Optimization (PPO) (Schulman et al., 2017b), which provides a first-order approximation to
194 the constrained optimization problems solved by TRPO and BPPO. This yields our final practical
195 loss function:

196
$$L^{MPPO} = \beta \mathbb{E}_{s \sim \rho_D(\cdot)} [\min(rA_{\pi_k}(s, a), \text{clip}(r, 1 - \epsilon, 1 + \epsilon)A_{\pi_k}(s, a))]$$
197
198
$$+ (1 - \beta) \mathbb{E}_{s \sim \rho_{\pi_k}(\cdot)} [\min(rA_{\pi_k}(s, a), \text{clip}(r, 1 - \epsilon, 1 + \epsilon)A_{\pi_k}(s, a))] \quad (4)$$
199

200 where ϵ restricts new π'_k from deviating from π_k , and $r = \frac{\pi'_k(a|s)}{\pi_k(a|s)}$ serves a dual purpose:
201

202

203 - **For the on-policy samples**, it acts as the **probability ratio**, quantifying the change in the
204 policy probability for a given action and forming the basis of the PPO clipping objective.
205 - **For the off-policy demonstration samples**, it functions both as the **probability ratio**
206 within the PPO objective and as the **importance sampling** mechanism to correct for the
207 distribution shift between the behavior policy and the current policy. This formulation pro-
208 vides an implicit constraint that anchors the updated policy π'_k to its immediate predecessor
209 π_k , which, due to small PPO updates, remains in the neighborhood of the teacher’s state-
210 action distribution. While BPPO introduces a decaying clipping ratio to further mitigate
211 distribution shift, we employ a small, fixed clipping value as a more simple and robust
212 alternative.

213

214 The mathematical unity of this term enables the seamless integration of offline and online data into
215 a consistent objective function. Thus, MPPO is guaranteed to improve the policy monotonically.
216 Next, we need to ensure the similarity between the student policy and the demonstration policy.

216 **Theorem 2.** π_T is the teacher’s policy, and π_S is the student’s policy. Given $D = \{\tau_1, \tau_2, \dots, \tau_N\}$,
 217 where each τ_i is sampled with π_T , the play style distance $D_{policy}(\pi_S, \pi_T)$ is non-increasing and is
 218 systematically guided toward the demonstrator’s policy under the influence of the offline component
 219 of MPPO, provided that $\forall (s_t, a_t) \in \tau_i$, the value $A_{\pi_T}(s_t, a_t)$ is positive¹.

220 Theorem 2 ensures that the policy is regularized to limit its divergence from the demonstrator’s
 221 policy. The MPPO objective (Eq. equation 4) primarily drives performance improvement, which
 222 may naturally lead the policy away from the teacher. The implicit constraint in Theorem 2 acts as
 223 a regularizer, anchoring the policy to the demonstrator’s behavioral style. The hyperparameter β
 224 governs the equilibrium between these dual objectives of proficiency and style consistency.

225 We have also modified the storage and replay mechanisms for the demonstration data in MPPO.
 226 Existing LfD and offline algorithms typically provide datasets as collections of (s, a, r) or
 227 (s, a, r, s', a') tuples. These methods either rely on 1-step TD estimation or require full processing
 228 and computation of entire trajectories to recover episodic information, which is necessary for multi-
 229 step TD or Monte Carlo-based advantage estimation. Additionally, a drawback of existing datasets
 230 is that complete state information must be stored, which often results in large storage footprints.

231 We collect demonstration trajectories τ_i by recording the environment initialization seed and action
 232 sequences $\{a_t\}_{t=0}^T$. During the training phase, complete episodes can be recovered by replaying
 233 these action sequences without modifying other online RL components. This enables full-episode
 234 advantage estimation methods, such as GAE, to be applied to both online and offline samples.

235 Building on the aforementioned results, we derive a practical algorithm. During training, two types
 236 of sampling actors are instantiated: 1) on-policy actors, which collect training data through environ-
 237 ment interactions using the latest student policy as described in the original PPO algorithm; and 2)
 238 LfD actors, which reproduce demonstrator data from the demonstration trajectories. To satisfy the
 239 conditions of Theorem 2, we filter trajectories from the dataset D , retaining only those with positive
 240 total returns for policy optimization. In particular, LfD actors initialize the game environment using
 241 the recorded seed and feed the action sequences to generate complete (s, a, r, v, adv) tuples as train-
 242 ing samples. Here, v denotes the state value estimated by the critic network, and adv represents the
 243 GAE advantage calculated from r and v . This approach ensures that data collected by both types of
 244 actors can be processed uniformly before being fed into the replay buffer for policy improvement.

245 To summarize, on the actor side, we modified the collection and replay mechanisms for offline data,
 246 enabling accurate full-episode advantage estimates to be readily applied to offline samples. On the
 247 learner side, theoretical results have established that MPPO can monotonically improve policies
 248 in both online and offline reinforcement learning settings. Additionally, MPPO’s behavior cloning
 249 constraint is implicitly defined between the demonstration policy π_T and the student policy π_S via
 250 data filtering. The pseudocode for MPPO is shown in Algorithm 1.

252 5 EXPERIMENTS

253 In this section, we aim to investigate two key questions: 1) **whether MPPO can meaningfully**
 254 **enhance agents’ game proficiency beyond suboptimal demonstrations**; and 2) **whether the im-**
 255 **proved agents can retain their game styles**.

256 We adopt the IMPALA architecture (Espeholt et al., 2018) for our experiments. At the end of each
 257 update step, the learner sends the latest model parameters to all actors, which then update their
 258 parameters before initiating new episodes. For MPPO agents in each environment, we adjusted the
 259 ratio of on-policy actors and LfD actors such that **demonstration data accounts for approximately**
 260 **5%** ($\beta = 0.05$) of the total incoming data.

261 We conduct experiments across three environments of varying scales: Blackjack, Maze, and MCR
 262 Mahjong. For each environment, we provide multiple suboptimal demonstrators, from which ap-
 263 proximately 30K demonstration trajectories with positive outcomes are collected per demonstrator.
 264 To compare storage footprints, we collect datasets in both our proposed format and the traditional
 265 format. Results show that our format reduces storage usage by 98%².

266 ¹The conclusion holds solely based on the positivity of $A_{\pi_T}(s_t, a_t)$, regardless of how A_{π_T} is defined or
 267 interpreted. The proof of the theorem is included in Appendix A

268 ²Blackjack: 1.13MB VS 84MB, Maze: 120MB VS 18.3GB, Mahjong: 155MB VS 40GB.

270 **Algorithm 1** Mixed Proximal Policy Optimization

271 **Input:** Collections of Demonstrations: $D = \{\tau_1, \tau_2, \dots, \tau_N\}$,

272 Actor policy: π_θ , Critic policy: V_ϕ , Demo Indicator: d

273

274 1: **for** $n=1,2,\dots$ **do**

275 2: **if** Demo Indicator $d \sim U(0, 1) < \beta$ **then**

276 3: sample $\tau_i = \{(s_t, a_t)\}_{t=0}^T \sim D$

277 4: Initialize environment

278 5: **for** $t=0,1,\dots,T$ **do**

279 6: retrieve action $a_t \in \{a_t\}_{t=0}^T$ from τ_i

280 7: estimate state value with V_ϕ

281 8: send trajectories with positive returns to learner

282 9: **end for**

283 10: **else**

284 11: Randomly initialize environment

285 12: **for** $t=0,1,\dots,T$ **do**

286 13: sample action $a_t \sim \pi_\theta$

287 14: estimate state value with V_ϕ

288 15: send all trajectories to learner

289 16: **end for**

290 17: **end if**

291 18: calculate advantage with GAE

292 19: update V_ϕ and π_θ with MPPO loss equation 4

293

294

295 Student agents are evaluated in terms of their game proficiency and their play style distance to their
 296 corresponding demonstrators. All experiments are repeated 5 times with different random seeds,
 297 and detailed experimental configurations for each environment are provided in Appendix C. Our
 298 anonymized data and codes are available at <https://github.com/AMysteriousBeing/MPPO>.

299 5.1 BLACKJACK

300

301 **Settings** Blackjack is a single agent stochastic game, and its rules and settings closely follow
 302 the descriptions in Sutton & Barto (2018). For players, the goal is to attain a hand closer to 21
 303 than the dealer’s without exceeding this value. We provide a rule-based Blackjack Bot A, whose
 304 policy is represented by the red dashed lines in Figure 1. We trained MPPO student agents using
 305 demonstration data from Bot A and compared their win rates with those of PPO agents, the optimal
 306 policy, and Bot A’s policy. A total of 15,000 fixed seeds are used to test the win rates of the rule-
 307 based bots and student agents.

308

309 **Results** As shown in Table 1A, the win rates of MPPO agents are comparable to those of the
 310 optimal policy and PPO agents, yet significantly higher than those of Bot A. Given the tractable state
 311 space of Blackjack, we can analyze agents’ game proficiency by examining their policy decision
 312 boundaries. As illustrated in Figure 1, MPPO agents consistently converge between the optimal
 313 policy and the demonstrator’s policy. This indicates that, in Blackjack, MPPO agents can surpass
 314 the game proficiency of the demonstrator while maintaining its play styles, an observation further
 315 supported by Table 1B. Specifically, MPPO agents’ policies are more distant from the optimal policy
 316 and closer to Bot A’s policy compared to PPO agents’ policies.

317 5.2 MAZE NAVIGATION

318

319 **Settings** The maze environment is a deterministic pathfinding task set in a 19×19 random grid
 320 world, where a valid path from the entrance to the exit is guaranteed. At each step within the maze,
 321 agents move in a single direction until they encounter a fork or a wall. The environment terminates
 322 under two conditions: if the agent reaches the exit, it receives a positive reward; if the step limit of
 323 80 is exceeded, no reward is given. Within the maze, the agent can observe 5 adjacent grids around
 its current position, and an example of a random maze is provided in Figure 2.

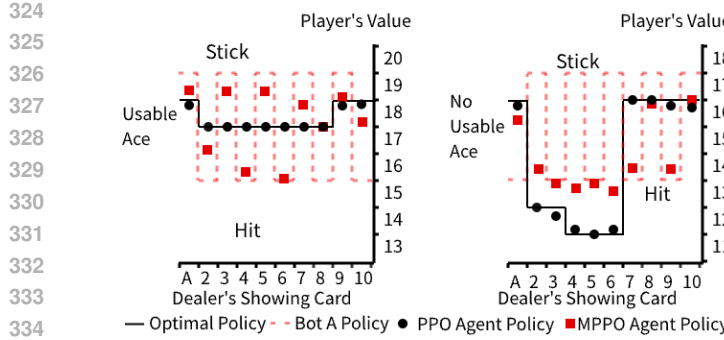


Figure 1: Visualization of Decision Boundaries Learned by PPO and MPPO Agents.

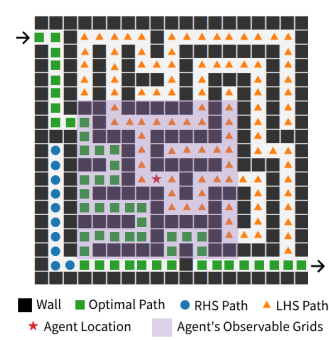


Figure 2: Example of a random maze.

Table 1: Blackjack A). Win rates and B). D_{policy} results

A	Optimal	Bot A	PPO Agent	MPPO Agent
	43.26	40.84	43.40 \pm 0.17	42.82 \pm 0.08
B	Optimal Policy	Bot A		
PPO	0.042 \pm 0.008		0.259 \pm 0.006	
MPPO	0.135 \pm 0.004		0.150 \pm 0.011	

Table 2: Maze A). Success Rates and B). D_{policy} Results.

A) Agents	Win Rate%	Avg Step
Optimal	100.00	25.224
Bot A	92.40	53.450
Bot B	89.00	55.714
PPO	99.64 \pm 0.12	27.230 \pm 0.147
MPPO A	99.52 \pm 0.31	27.649 \pm 0.440
MPPO B	99.04 \pm 0.81	28.104 \pm 0.649

B) Agents	Optimal	Bot A	Bot B
PPO	.057 \pm .002	.509 \pm .002	.492 \pm .001
MPPO A	.084 \pm .001	.471 \pm .013	.530 \pm .008
MPPO B	.076 \pm .004	.521 \pm .010	.481 \pm .009

Table 3: Mahjong's Bot Information

Bot Name	UUID	Ranking	Elo Score
Baseline	5eb7...123e	1	1328.76
Bot A	5fdf...5837	17	1240.50
Bot B	627e...c460	161	1128.66
Bot C	5ecc...eb73	266	980.51

For maze-navigating bots, we provide Maze Bot A, a right-hand search (RHS) bot, and Maze Bot B, a left-hand search (LHS) bot. The RHS and LHS bots implement right-hand and left-hand wall-following behaviors, respectively. For the maze environment, we use success rates and average steps to quantify agents' proficiency. A run is considered successful if the agent reaches the exit within the step limit. We evaluated agents in 500 unseen mazes.

Results As shown in Table 2A, the success rates of MPPO agents are comparable to those of PPO agents, yet MPPO agents require slightly more steps on average to exit the mazes. In contrast to their demonstrators, MPPO agents exhibit significantly higher success rates, with their average steps reduced by approximately 20.

For the D_{policy} metric, Table 2B demonstrates that MPPO achieves meaningful policy improvement while preserving the navigation styles of its demonstrators. This can be explained by the strategies learned by the agents. The MPPO A agent, while converging to a near-optimal policy, retains a stylistic preference for right-hand turns inherited from its demonstrator (Maze Bot A). Analytically, this is reflected in its policy logits, which show a stronger propensity for right turns compared to the PPO agent when facing ambiguous states (as the environment is partially observable). Behaviorally, this bias manifests as more occasional detours to the right in certain maze configurations, which directly accounts for the slightly increased average path length in Table 2A. The same principle explains the results for MPPO B, which exhibits a symmetric preference for left-hand turns.

5.3 MAHJONG

Settings Mahjong is a multi-player game with imperfect information. The complexity of imperfect-information games can be quantified by information sets (info sets), which refer to game

378 states that players are unable to differentiate based on their observations. Mahjong features around
 379 10^{121} info sets, with the average size of each set estimated at 10^{48} , a complexity vastly exceeding
 380 that of Heads-Up Texas Hold'em, where the average info set size is roughly 10^3 (Lu et al., 2023).
 381

382 The game is played with a set of 144 tiles. Each player begins with 13 tiles, which are only observ-
 383 able by themselves. They take turns to draw and discard a tile until one completes a winning hand
 384 with a 14th tile. Our environment adopts the Mahjong Competition Rules (MCR) variant, which
 385 contains 81 different scoring patterns. The details of the MCR are provided in Appendix B.
 386

387 For the Mahjong environment, we additionally analyze the distribution of winning patterns between
 388 agents, as these patterns reflect the strategies employed by the winners during the game. We denote
 389 the distance between winning pattern distributions as D_{target} , defined in equation 5. Here, p denotes
 390 an MCR pattern, P represents the set of all patterns, and $\pi_i(p)$ refers to the probability that an
 391 agent following policy π_i wins with pattern p . Compared to D_{policy} , D_{target} provides a more
 392 straightforward measure of play style, enabling us to examine whether micro-level play styles indeed
 393 influence macro-level strategies.
 394

$$393 \quad D_{target} = \frac{1}{2} \sum_{p \in P} |\pi_1(p) - \pi_2(p)| \quad (5)$$

396 The MCR Mahjong bots are selected from Botzone (Zhou et al., 2018), an online platform for AI in
 397 games. As shown in Table 3, the demonstrators, specifically Bot A, B, and C, are deliberately chosen
 398 from different performance ranges. For reference, currently there are over 600 bots on the platform,
 399 and Elo scores range from 460 to 1328. To accelerate training, MPPO and PPO agents (A, B, and
 400 C) are initialized using behavior cloning checkpoints derived from Bot A, B, and C, respectively³.
 401

402 All student agents are evaluated for game proficiency against the Baseline bot every 12 hours. The
 403 win rates of the demonstrator bots are calculated directly from Botzone's historical Elo data. Mean-
 404 while, the win rate of each student agent is determined by testing the agent against the baseline bot
 405 over 512 games. We use the final checkpoints of the agents to calculate D_{policy} . For the action dis-
 406 tributions of the demonstrator bots, we collect (s, a) pairs from 100 trajectories **not** used in training,
 407 and we set $p(a|s) = \mathbf{1}_{a=a_i}, \forall a_i \in A$. We exclude states s with only one legal action and feed the re-
 408 maining states into the agents' models. Similarly, for D_{target} , the winning pattern distribution $\pi(p)$
 409 of the demonstrator bots is calculated directly from their historical game data, whereas the $\pi(p)$ of
 410 student agents is derived from policy evaluation runs using 20,000 fixed seeds.
 411

411 Table 4: Mahjong A). Win Rates and B). D_{policy}
 412 Results.

A) Win Rate	Teacher	MPPO	PPO
VS Base	Bot	Agents	Agents
Bot A	43.67	51.05±1.43	36.72±3.11
Bot B	39.82	46.17±1.72	34.96±2.57
Bot C	37.05	42.42±3.66	33.32±1.41

B) D_{policy}	MPPO	PPO	Bot B	Bot A	Bot B	Bot C
Bot A	0.297±.016	0.678±.027	PPO B	0.201±.007	.214±.007	.221±.008
Bot B	0.318±.007	0.691±.013	MPPO B	0.047±.007	.039±.005	.068±.004
Bot C	0.279±.020	0.772±.027	Bot C	.071	0.063	0

411 Table 5: D_{target} between teachers and students.
 412 Values between student and demonstrator pairs
 413 are highlighted.

D_{target}	Bot A	Bot B	Bot C
Bot A	0	.023	.071
Bot B	.195±.003	.208±.003	.215±.004
Bot C	.037±.008	.047±.009	.077±.002

	Bot B	Bot A	PPO C	MPPO C
Bot B	.023	0	.063	
Bot A	.071	0.063	0	
PPO C	.191±.006	.204±.007	.212±.007	
MPPO C	.086±.002	.076±.010	.047±.012	

425 **Results** The performance of agents against the baseline is presented in Figure 3. MPPO agents
 426 quickly surpass their demonstrators, and Bot A student agents defeat the baseline at the end of train-
 427 ing. We recorded the best performance of each student agent across all runs, and the results are
 428 summarized in Table 4A. For reference, the champion bot from the IJCAI 2024 Mahjong AI Com-
 429 petition ranks 33rd in Botzone's Elo rankings. This indicates that MPPO agents can outperform
 430

431 ³This warm-start is employed solely to reduce wall-clock time and resource consumption and is not a
 432 methodological prerequisite, as shown in Appendix G.

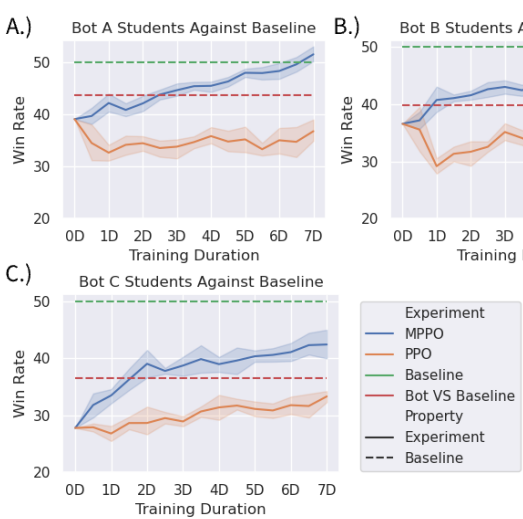


Figure 3: Bots’ win rates against the Baseline. Red dashed lines are the demonstrators’ win rates against Baseline. Shaded areas are 95% confidence intervals.

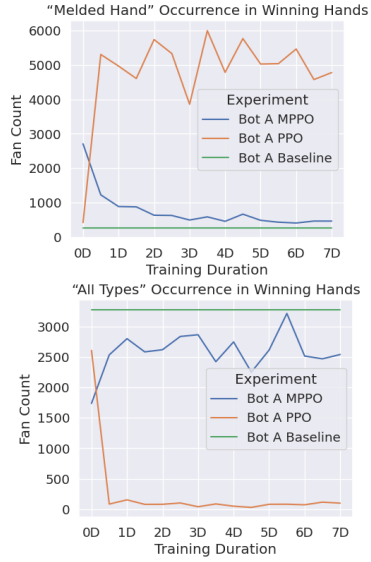


Figure 4: Occurrence of selected patterns.

top-tier bots using suboptimal demonstrations. As shown in Table 4B, the D_{policy} values of student agents relative to their demonstrator bots indicate that MPPO agents have action distributions significantly closer to their demonstrator bots than PPO agents.

In Table 5, the D_{target} values between MPPO student agents and their corresponding demonstrators are consistently the lowest, confirming the observation from D_{policy} . Additionally, Bot A and Bot B have relatively close target distributions, and this proximity in target preference is also inherited by MPPO agents A and B.

In the calculation of D_{target} , we observe that PPO agents rapidly lose the ability to achieve some patterns while focusing on several others. In contrast, MPPO agents retain the ability to achieve most patterns, a capability preserved by the demonstration trajectories, as illustrated in Figure 4. This phenomenon explains why the D_{target} values of PPO agents are significantly higher than those of MPPO agents.

Now we can address the questions posed at the beginning of this section. MPPO exhibits a strong ability to surpass the proficiency of demonstrators and, in some cases, even outperform PPO. By comparing D_{policy} values among PPO agents, MPPO agents, and bots, we conclude that MPPO agents imitate the play styles of their demonstrators at the action level. Further analysis of D_{target} in Mahjong confirms that such action-level style similarities extend to the strategy level, for example, target selection in MCR Mahjong, and that MPPO agents thus retain their demonstrators’ play styles.

6 ABLATION AND COMPARATIVE STUDY

To analyze the impact of different components of the MPPO algorithm, we conducted ablation studies using Bot A’s trajectories across each environment. Table 6 summarizes the win rates and D_{policy} values between the agent groups and their corresponding demonstrators⁴.

For the **2x Demo** and **0.5x Demo** experiments, we doubled and halved the value of β , respectively, to analyze the impact of the demonstration data ratio. As expected, a higher ratio of demonstration data leads to a lower D_{policy} . The proportion of demonstration data also affects the final proficiency of the agents. In each environment, the proficiency metrics of MPPO agents peak at different ratios, indicating that different environments correspond to unique optimal ratios of demonstration data.

⁴The learning curves are presented in Appendix C.

486
 487 Table 6: Summarized ablation and comparison study results for A) Win rates and B) D_{policy} with
 488 each environment’s Bot A. Ablation and comparative study results are separated by a horizontal line.
 489 Highest Win rates and lowest D_{policy} values in ablation study results are highlighted.

Method	A)	Blackjack	Maze	Mahjong	B)	Blackjack	Maze	Mahjong
PPO	43.40±0.17	99.64±0.12	36.72±3.11		.259±.006	.509±.002	.678±.027	
MPPO Ref	42.82±0.08	99.52±0.31	51.05±1.43		.150±.011	.471±.013	.297±.016	
2x Demo	42.08±0.06	99.60±0.20	48.09±1.86		.093±.007	.457±.018	.287±.006	
0.5x Demo	42.93±0.12	99.12±0.99	46.84±1.97		.186±.003	.492±.012	.324±.007	
All Data	43.62±0.04	94.24±0.81	42.30±3.65		.294±.003	.572±.016	.775±.057	
TD(0) Adv	43.31±0.28	99.40±0.69	17.34±0.74		.218±.004	.523±.003	.727±.042	
GAIL	25.63±1.21	92.40±0.00	3.32±0.58		.501±.010	2e-6 ± 0	.784±.044	
SAIL	38.50±0.01	94.52±0.70	19.73±3.30		.495±.006	.540±.017	.690±.025	
DQfD	42.26±0.29	87.20±2.62	15.43±1.38		.411±.003	.659±.001	.793±.004	
PPOfD	42.89±0.15	99.40±0.20	41.52±2.59		.231±.011	.347±.009	.335±.019	

500
 501
 502 For the **All Data** experiments, we regenerate all datasets to include all trajectories for demonstration.
 503 This violates the prerequisite condition $A_\pi(s_t, a_t) > 0$ in Theorem 2, reducing the entire algorithm
 504 to online PPO where a fraction of the actors sample from fixed seed environments with a fixed policy.
 505 In this setting, D_{policy} values are high in all environments, and the win rates vary by environment.

506 For the **TD(0) Adv** experiments, we replace GAE with 1-step TD advantage, an approach com-
 507 monly adopted in existing offline RL and LfD methods. This weakens the prerequisite condition
 508 $A_\pi(s_t, a_t) > 0$ in Theorem 2, since 1-step TD responds slowly to the final reward. Consequently,
 509 we observe higher D_{policy} values in all settings. While TD(0) performs well in Blackjack and Maze,
 510 it struggles in Mahjong, a more complex environment with long-horizon decision sequences, as it
 511 fails to leverage all future information.

512 For the comparative study, we compare MPPO with other LfD and IL methods: GAIL, SAIL, and
 513 DQfD. As shown in Table 6A, GAIL and SAIL perform well in Maze, a 2D state-space environment,
 514 yet struggle in Mahjong, where defining similarity between state-action pairs is challenging. This
 515 aligns with the findings of Brown et al. (2019), which note that adversarial-based IL methods do not
 516 scale effectively to high-dimensional scenarios.

517 DQfD also performs poorly in Mahjong: its training trajectories for the game exhibit the same low-
 518 entropy characteristics as those of the MPPO algorithm. To eliminate the influence of backbone
 519 algorithms and differences in action-sampling strategies, we ported DQfD’s explicit supervised loss
 520 to MPPO, creating *PPOfD*. In essence, PPOfD differs from MPPO solely in the mechanism by
 521 which it encourages students to imitate demonstrators. PPOfD outperforms DQfD across all envi-
 522 ronments; it is comparable to MPPO in Blackjack and Maze but lags significantly behind MPPO in
 523 Mahjong. This indicates that our implicit behavior cloning constraint is more adaptable to diverse
 524 environments than explicit loss functions.

525 Regarding play styles, as shown in Table 6B, MPPO is the only method that meaningfully maintains
 526 low D_{policy} values while improving agent proficiency across all environments.
 527

529 7 CONCLUSION

531 In this paper, we tackle the dual objectives of proficiency and diversity in game-playing agents
 532 through MPPO, a method that enhances the proficiency of suboptimal agents while preserving their
 533 play styles. Through theoretical analysis, MPPO unifies the loss objectives for both online and of-
 534 fline samples, and implicitly guides student agents toward the demonstrators’ policies by adjusting
 535 the empirical distribution of samples. Our experiments show that MPPO matches or even outper-
 536 forms the pure online baseline (PPO) in proficiency, while preserving demonstrators’ game styles
 537 by closely aligning with their policy distributions. Looking ahead, we aim to extend our method to
 538 continuous action domains. In addition, exploring trajectory-level metrics, such as state visitation
 539 distributions, presents a promising path for a richer characterization of behavioral style. We expect
 this work to contribute to more engaging gameplay and a more diverse agent ecosystem.

540 REFERENCES

542 Adrià Puigdomènech Badia, Bilal Piot, Steven Kapturowski, Pablo Sprechmann, Alex Vitvitskyi,
 543 Daniel Guo, and Charles Blundell. Agent57: Outperforming the atari human benchmark, 2020.
 544 URL <https://arxiv.org/abs/2003.13350>.

545 Philip J. Ball, Laura Smith, Ilya Kostrikov, and Sergey Levine. Efficient online reinforcement learning with offline data, 2023. URL <https://arxiv.org/abs/2302.02948>.

546 Pablo Barros, Özge Nilay Yalçın, Ana Tanevska, and Alessandra Sciutti. Incorporating rivalry in
 547 reinforcement learning for a competitive game. *Neural Computing and Applications*, 35(23):
 548 16739–16752, Aug 2023. ISSN 1433-3058. doi: 10.1007/s00521-022-07746-9. URL <https://doi.org/10.1007/s00521-022-07746-9>.

549 Christopher Berner, Greg Brockman, Brooke Chan, Vicki Cheung, Przemyslaw Debiak, Christy
 550 Dennison, David Farhi, Quirin Fischer, Shariq Hashme, Christopher Hesse, Rafal Józefowicz,
 551 Scott Gray, Catherine Olsson, Jakub Pachocki, Michael Petrov, Henrique Pondé de Oliveira Pinto,
 552 Jonathan Raiman, Tim Salimans, Jeremy Schlatter, Jonas Schneider, Szymon Sidor, Ilya
 553 Sutskever, Jie Tang, Filip Wolski, and Susan Zhang. Dota 2 with large scale deep reinforcement
 554 learning. *CoRR*, abs/1912.06680, 2019. URL <http://arxiv.org/abs/1912.06680>.

555 Daniel S. Brown, Wonjoon Goo, Prabhat Nagarajan, and Scott Niekum. Extrapolating beyond
 556 suboptimal demonstrations via inverse reinforcement learning from observations, 2019. URL
 557 <https://arxiv.org/abs/1904.06387>.

558 Rodrigo Canaan, Julian Togelius, Andy Nealen, and Stefan Menzel. Diverse agents for ad-hoc
 559 cooperation in hanabi, 2019. URL <https://arxiv.org/abs/1907.03840>.

560 Jessica Chemali and Alessandro Lazaric. Direct policy iteration with demonstrations. In *Proceed-
 561 ings of the 24th International Conference on Artificial Intelligence*, IJCAI’15, pp. 3380–3386.
 562 AAAI Press, 2015. ISBN 9781577357384.

563 Stephen Chen. *Learning player behavior models to enable cooperative planning for non-player
 564 characters*. PhD thesis, Carnegie Mellon University Pittsburgh, PA, 2017.

565 Zefeng Chen, Yuren Zhou, Xiaoyu He, and Siyu Jiang. A restart-based rank-1 evolution strategy for
 566 reinforcement learning. In *Proceedings of the 28th International Joint Conference on Artificial
 567 Intelligence*, IJCAI’19, pp. 2130–2136. AAAI Press, 2019. ISBN 9780999241141.

568 Laura Climent, Alessio Longhi, Alejandro Arbelaez, and Maurizio Mancini. A framework for de-
 569 signing reinforcement learning agents with dynamic difficulty adjustment in single-player action
 570 video games. *Entertainment Computing*, 50:100686, 2024. ISSN 1875-9521. doi: <https://doi.org/10.1016/j.entcom.2024.100686>. URL <https://www.sciencedirect.com/science/article/pii/S1875952124000545>.

571 Lasse Espeholt, Hubert Soyer, Rémi Munos, Karen Simonyan, Volodymyr Mnih, Tom Ward, Yotam
 572 Doron, Vlad Firoiu, Tim Harley, Iain Dunning, Shane Legg, and Koray Kavukcuoglu. IMPALA:
 573 scalable distributed deep-rl with importance weighted actor-learner architectures. *CoRR*,
 574 abs/1802.01561, 2018. URL <http://arxiv.org/abs/1802.01561>.

575 Lior Fuks, Noor Awad, Frank Hutter, and Marius Lindauer. An evolution strategy with pro-
 576 gressive episode lengths for playing games. In *Proceedings of the Twenty-Eighth International
 577 Joint Conference on Artificial Intelligence*, IJCAI-19, pp. 1234–1240. International Joint Con-
 578 ferences on Artificial Intelligence Organization, 7 2019. doi: 10.24963/ijcai.2019/172. URL
 579 <https://doi.org/10.24963/ijcai.2019/172>.

580 Yiming Gao, Feiyu Liu, Liang Wang, Zhenjie Lian, Weixuan Wang, Siqin Li, Xianliang Wang,
 581 Xianhan Zeng, Rundong Wang, Jiawei Wang, Qiang Fu, Wei Yang, Lanxiao Huang, and Wei Liu.
 582 Towards effective and interpretable human-agent collaboration in moba games: A communication
 583 perspective, 2023. URL <https://arxiv.org/abs/2304.11632>.

584 Ian J. Goodfellow, Jean Pouget-Abadie, Mehdi Mirza, Bing Xu, David Warde-Farley, Sherjil Ozair,
 585 Aaron Courville, and Yoshua Bengio. Generative adversarial networks, 2014. URL <https://arxiv.org/abs/1406.2661>.

594 Todd Hester, Matej Vecerík, Olivier Pietquin, Marc Lanctot, Tom Schaul, Bilal Piot, Andrew
 595 Sendonaris, Gabriel Dulac-Arnold, Ian Osband, John P. Agapiou, Joel Z. Leibo, and Au-
 596 drunas Gruslys. Learning from demonstrations for real world reinforcement learning. *CoRR*,
 597 abs/1704.03732, 2017. URL <http://arxiv.org/abs/1704.03732>.

598 Jonathan Ho and Stefano Ermon. Generative adversarial imitation learning. *CoRR*, abs/1606.03476,
 599 2016. URL <http://arxiv.org/abs/1606.03476>.

600 Muhan Hou, Koen Hindriks, Gusztí Eiben, and Kim Baraka. “give me an example like this”:
 601 Episodic active reinforcement learning from demonstrations. In *Proceedings of the 12th Inter-
 602 national Conference on Human-Agent Interaction*, HAI ’24, pp. 287–295, New York, NY, USA,
 603 2024. Association for Computing Machinery. ISBN 9798400711787. doi: 10.1145/3687272.
 604 3688298. URL <https://doi.org/10.1145/3687272.3688298>.

605 Yuhua Jiang, Qihan Liu, Xiaoteng Ma, Chenghao Li, Yiqin Yang, Jun Yang, Bin Liang, and
 606 Qianchuan Zhao. Learning diverse risk preferences in population-based self-play, 2023. URL
 607 <https://arxiv.org/abs/2305.11476>.

608 Sham Kakade and John Langford. Approximately optimal approximate reinforcement learning. In
 609 *Proceedings of the Nineteenth International Conference on Machine Learning*, ICML ’02, pp.
 610 267–274, San Francisco, CA, USA, 2002. Morgan Kaufmann Publishers Inc. ISBN 1558608737.

611 Bingyi Kang, Zequn Jie, and Jiashi Feng. Policy optimization with demonstrations. In Jennifer
 612 Dy and Andreas Krause (eds.), *Proceedings of the 35th International Conference on Machine
 613 Learning*, volume 80 of *Proceedings of Machine Learning Research*, pp. 2469–2478. PMLR,
 614 10–15 Jul 2018. URL <https://proceedings.mlr.press/v80/kang18a.html>.

615 Joel Lehman and Kenneth O. Stanley. Evolving a diversity of virtual creatures through novelty
 616 search and local competition. In *Proceedings of the 13th Annual Conference on Genetic and
 617 Evolutionary Computation*, GECCO ’11, pp. 211–218, New York, NY, USA, 2011. Associa-
 618 tion for Computing Machinery. ISBN 9781450305570. doi: 10.1145/2001576.2001606. URL
 619 <https://doi.org/10.1145/2001576.2001606>.

620 Chiu-Chou Lin, Wei-Chen Chiu, and I-Chen Wu. Perceptual similarity for measuring decision-
 621 making style and policy diversity in games. *Transactions on Machine Learning Research*, 2024.
 622 ISSN 2835-8856. URL <https://openreview.net/forum?id=30C9AWBW49>.

623 Yunlong Lu, Wenxin Li, and Wenlong Li. Official international mahjong: A new playground for ai
 624 research. *Algorithms*, 16(5), 2023. ISSN 1999-4893. doi: 10.3390/a16050235. URL <https://www.mdpi.com/1999-4893/16/5/235>.

625 Volodymyr Mnih, Koray Kavukcuoglu, David Silver, Alex Graves, Ioannis Antonoglou, Daan
 626 Wierstra, and Martin Riedmiller. Playing atari with deep reinforcement learning, 2013. URL
 627 <https://arxiv.org/abs/1312.5602>.

628 Ashvin Nair, Abhishek Gupta, Murtaza Dalal, and Sergey Levine. Awac: Accelerating online re-
 629 inforcement learning with offline datasets, 2021. URL <https://arxiv.org/abs/2006.09359>.

630 Mitsuhiko Nakamoto, Yuxiang Zhai, Anikait Singh, Max Sobol Mark, Yi Ma, Chelsea Finn, Aviral
 631 Kumar, and Sergey Levine. Cal-ql: Calibrated offline rl pre-training for efficient online fine-
 632 tuning, 2024. URL <https://arxiv.org/abs/2303.05479>.

633 Jack Parker-Holder, Aldo Pacchiano, Krzysztof Choromanski, and Stephen Roberts. Effective di-
 634 versity in population based reinforcement learning, 2020. URL <https://arxiv.org/abs/2002.00632>.

635 Diego Perez-Liebana, Yu-Jhen Hsu, Stavros Emmanouilidis, Bobby Khaleque, and Raluca Gaina.
 636 Tribes: A new turn-based strategy game for ai research. *Proceedings of the AAAI Conference on
 637 Artificial Intelligence and Interactive Digital Entertainment*, 16(1):252–258, Oct. 2020. doi: 10.
 638 1609/aiide.v16i1.7438. URL <https://ojs.aaai.org/index.php/AIIDE/article/view/7438>.

648 Bilal Piot, Matthieu Geist, and Olivier Pietquin. Boosted bellman residual minimization handling
 649 expert demonstrations. In Toon Calders, Floriana Esposito, Eyke Hüllermeier, and Rosa Meo
 650 (eds.), *Machine Learning and Knowledge Discovery in Databases*, pp. 549–564, Berlin, Heidel-
 651 berg, 2014. Springer Berlin Heidelberg. ISBN 978-3-662-44851-9.

652

653 Edwin A. Romero-Mendez, Pedro C. Santana-Mancilla, Miguel Garcia-Ruiz, Osval A. Montesinos-
 654 López, and Luis E. Anido-Rifón. The use of deep learning to improve player engagement in
 655 a video game through a dynamic difficulty adjustment based on skills classification. *Applied
 656 Sciences*, 13(14), 2023. ISSN 2076-3417. doi: 10.3390/app13148249. URL <https://www.mdpi.com/2076-3417/13/14/8249>.

657

658 John Schulman, Philipp Moritz, Sergey Levine, Michael I. Jordan, and P. Abbeel. High-dimensional
 659 continuous control using generalized advantage estimation. *CoRR*, abs/1506.02438, 2015. URL
 660 <https://api.semanticscholar.org/CorpusID:3075448>.

661

662 John Schulman, Sergey Levine, Philipp Moritz, Michael I. Jordan, and Pieter Abbeel. Trust region
 663 policy optimization, 2017a. URL <https://arxiv.org/abs/1502.05477>.

664

665 John Schulman, Filip Wolski, Prafulla Dhariwal, Alec Radford, and Oleg Klimov. Proximal policy
 666 optimization algorithms. *CoRR*, abs/1707.06347, 2017b. URL <http://arxiv.org/abs/1707.06347>.

667

668 David Silver, Thomas Hubert, Julian Schrittwieser, Ioannis Antonoglou, Matthew Lai, Arthur Guez,
 669 Marc Lanctot, Laurent Sifre, Dharshan Kumaran, Thore Graepel, Timothy P. Lillicrap, Karen
 670 Simonyan, and Demis Hassabis. Mastering chess and shogi by self-play with a general reinforce-
 671 ment learning algorithm. *CoRR*, abs/1712.01815, 2017. URL <http://arxiv.org/abs/1712.01815>.

672

673 Richard S. Sutton and Andrew G. Barto. *Reinforcement Learning: An Introduction*. A Bradford
 674 Book, Cambridge, MA, USA, 2018. ISBN 0262039249.

675

676 John Sweller. Cognitive load theory, learning difficulty, and instructional design. *Learn-
 677 ing and Instruction*, 4(4):295–312, 1994. ISSN 0959-4752. doi: [https://doi.org/10.1016/0959-4752\(94\)90003-5](https://doi.org/10.1016/0959-4752(94)90003-5). URL <https://www.sciencedirect.com/science/article/pii/0959475294900035>.

678

679

680 Zhenggang Tang, Chao Yu, Boyuan Chen, Huazhe Xu, Xiaolong Wang, Fei Fang, Simon Du,
 681 Yu Wang, and Yi Wu. Discovering diverse multi-agent strategic behavior via reward random-
 682 ization, 2021. URL <https://arxiv.org/abs/2103.04564>.

683

684 Leonid Nisonovich Vaserstein. Markov processes over denumerable products of spaces, describing
 685 large systems of automata. *Problemy Peredachi Informatsii*, 5(3):64–72, 1969.

686

687 Matej Vecerík, Todd Hester, Jonathan Scholz, Fumin Wang, Olivier Pietquin, Bilal Piot, Nico-
 688 las Heess, Thomas Rothörl, Thomas Lampe, and Martin A. Riedmiller. Leveraging demon-
 689 strations for deep reinforcement learning on robotics problems with sparse rewards. *CoRR*,
 690 abs/1707.08817, 2017. URL <http://arxiv.org/abs/1707.08817>.

691

692 Oriol Vinyals, Igor Babuschkin, Wojciech M. Czarnecki, Michaël Mathieu, Andrew Dudzik, Juny-
 693 oung Chung, David H. Choi, Richard Powell, Timo Ewalds, Petko Georgiev, Junhyuk Oh, Dan
 694 Horgan, Manuel Kroiss, Ivo Danihelka, Aja Huang, Laurent Sifre, Trevor Cai, John P. Aga-
 695 piou, Max Jaderberg, Alexander S. Vezhnevets, Rémi Leblond, Tobias Pohlen, Valentin Dalibard,
 696 David Budden, Yury Sulsky, James Molloy, Tom L. Paine, Caglar Gulcehre, Ziyu Wang, To-
 697 bias Pfaff, Yuhuai Wu, Roman Ring, Dani Yogatama, Dario Wünsch, Katrina McKinney, Oliver
 698 Smith, Tom Schaul, Timothy Lillicrap, Koray Kavukcuoglu, Demis Hassabis, Chris Apps, and
 699 David Silver. Grandmaster level in starcraft ii using multi-agent reinforcement learning. *Na-
 700 ture*, 575(7782):350–354, Nov 2019. ISSN 1476-4687. doi: 10.1038/s41586-019-1724-z. URL
 701 <https://doi.org/10.1038/s41586-019-1724-z>.

702

703 Andrew Wagenmaker and Aldo Pacchiano. Leveraging offline data in online reinforcement learning,
 704 2023. URL <https://arxiv.org/abs/2211.04974>.

702 Guan Yang, Minghuan Liu, Weijun Hong, Weinan Zhang, Fei Fang, Guangjun Zeng, and Yue Lin.
 703 Perfectdou: Dominating doudizhu with perfect information distillation, 2024. URL <https://arxiv.org/abs/2203.16406>.
 704

705 Deheng Ye, Guibin Chen, Wen Zhang, Sheng Chen, Bo Yuan, Bo Liu, Jia Chen, Zhao Liu, Fuhan
 706 Qiu, Hongsheng Yu, Yinyuting Yin, Bei Shi, Liang Wang, Tengfei Shi, Qiang Fu, Wei Yang,
 707 Lanxiao Huang, and Wei Liu. Towards playing full MOBA games with deep reinforcement learn-
 708 ing. *CoRR*, abs/2011.12692, 2020. URL <https://arxiv.org/abs/2011.12692>.
 709

710 Maryam Zare, Parham M. Kebria, Abbas Khosravi, and Saeid Nahavandi. A survey of imitation
 711 learning: Algorithms, recent developments, and challenges. *IEEE Transactions on Cybernetics*,
 712 54(12):7173–7186, 2024. doi: 10.1109/TCYB.2024.3395626.

713 Enmin Zhao, Renye Yan, Jinqiu Li, Kai Li, and Junliang Xing. Alphaholdem: High-performance
 714 artificial intelligence for heads-up no-limit poker via end-to-end reinforcement learning. *Pro-
 715 ceedings of the AAAI Conference on Artificial Intelligence*, 36(4):4689–4697, Jun. 2022. doi: 10.
 716 1609/aaai.v36i4.20394. URL <https://ojs.aaai.org/index.php/AAAI/article/view/20394>.
 717

718 Haoyu Zhou, Haifeng Zhang, Yushan Zhou, Xinchao Wang, and Wenxin Li. Botzone: an online
 719 multi-agent competitive platform for ai education. In *Proceedings of the 23rd Annual ACM Con-
 720 ference on Innovation and Technology in Computer Science Education*, ITiCSE 2018, pp. 33–38,
 721 New York, NY, USA, 2018. Association for Computing Machinery. ISBN 9781450357074. doi:
 722 10.1145/3197091.3197099. URL <https://doi.org/10.1145/3197091.3197099>.
 723

724 Zhuangdi Zhu, Kaixiang Lin, Bo Dai, and Jiayu Zhou. Learning sparse rewarded tasks from sub-
 725 optimal demonstrations. *CoRR*, abs/2004.00530, 2020. URL <https://arxiv.org/abs/2004.00530>.
 726

727 Zifeng Zhuang, Kun Lei, Jinxin Liu, Donglin Wang, and Yilang Guo. Behavior proximal policy
 728 optimization, 2023. URL <https://arxiv.org/abs/2302.11312>.
 729

730 A PROOF OF THEOREM 2

732 *Proof.* We study the effect of MPPO’s offline objective when clipping is not activated. Define
 733 $\mathbf{1}_{a=x}$ as 1 if action $a = x$, else 0, then $\pi_T(a|s_t) = \mathbf{1}_{a=a_t}$. Then $\forall (s_t, a_t) \in \tau_i$, the next iteration
 734 policy $\pi'_S(a_t|s_t) = \pi_S(a_t|s_t) + \alpha \frac{\nabla \pi_S(a_t|s_t)}{\pi_T(a_t|s_t)} A_{\pi_T}(s_t, a_t)$, where α is a constant. The change in
 735 $2D_{policy}(\pi_S, \pi_T) = \sum_a |\pi_T(a|s_t), \pi_S(a|s_t)|$ is:
 736

$$\begin{aligned} \sum_a (|\pi_T(a|s_t), \pi'_S(a|s_t)| - |\pi_T(a|s_t), \pi_S(a|s_t)|) &= \sum_{a=a_t} (\pi_S(a|s_t) - \pi'_S(a|s_t)) + \sum_{a \neq a_t} (\pi'_S(a|s_t) - \pi_S(a|s_t)) \\ &= \pi_S(a_t|s_t) - \pi'_S(a_t|s_t) + \pi_S(a_t|s_t) - \pi'_S(a_t|s_t) = -2\alpha \frac{\nabla \pi_S(a_t|s_t)}{\mathbf{1}_{a=a_t}} A_{\pi_T}(s_t, a_t) \\ &- \alpha \frac{\nabla \pi_S(a_t|s_t)}{\mathbf{1}_{a=a_t}} A_{\pi_T} < 0 \text{ as } \alpha > 0, \text{ thus } D_{policy}(\pi_S, \pi_T) \text{ decreases as training progresses if } A_{\pi_T} \text{ is positive.} \end{aligned}$$

□

744 B MCR MAHJONG ENVIRONMENT DESCRIPTION

747 Mahjong is a four-player tile-based tabletop game involving imperfect information. The complexity
 748 of imperfect-information games can be quantified by information sets, which refer to game states that
 749 players are unable to differentiate based on their own observations. The average size of information
 750 sets in Mahjong is approximately 10^{48} , rendering it a considerably more complex game to solve
 751 compared to Heads-Up Texas Hold’em, where the average size of information sets is around 10^3 .
 752 To enhance the readability of this paper, we highlight the terminologies used in Mahjong with **bold**
 753 **texts**, and we differentiate scoring patterns with *italicized texts*.

754 In Mahjong, there are 144 tiles, as depicted in Figure 5A. Despite the existence of numerous rule
 755 variants, the general rules of Mahjong remain the same. At a broad level, Mahjong is a pattern-
 matching game. Each player starts with 13 tiles that are only visible to themselves, and they take

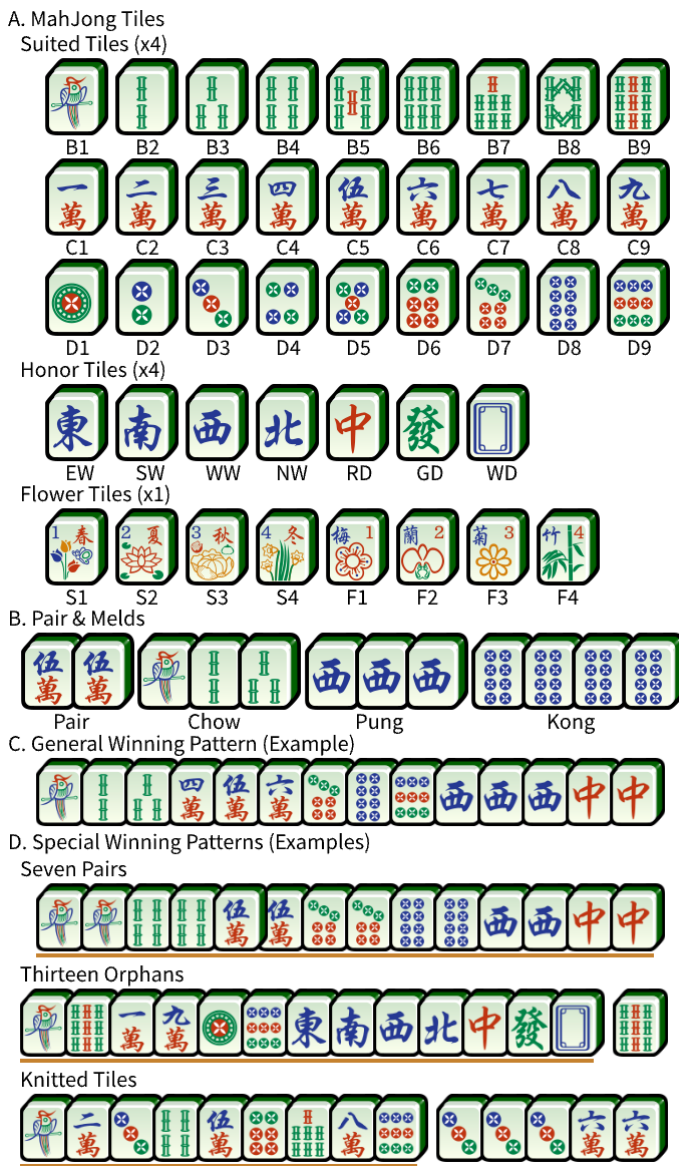


Figure 5: Basics of Mahjong. A). All the Mahjong tiles. There are four identical copies for each tile. B). Examples of Chow, Pung, and Kong. Only suited tiles are available for Chow. C). Example of the GWP. D). Examples of special winning patterns, the special patterns are separated and underscored.

turns to draw and discard one tile until one completes a winning pattern with a 14th tile. The general winning pattern (GWP) of 14 tiles consists of four **melds** and a **pair**, as shown in Fig. 5C. A **meld** can be in the form of **Chow**, **Pung**, or **Kong**, as shown in Fig. 5B. Besides drawing all the tiles by themselves, players have the option to take the tile just discarded by another player instead of drawing one to form a **meld** or declare a win.

B.1 OFFICIAL INTERNATIONAL MAHJONG

Official International Mahjong, also known as Mahjong Competition Rules (MCR), is a Mahjong variant aiming to enhance the game's complexity and competitiveness while weakening its gambling nature. It specifies 81 scoring patterns, which range from 1 to 88 points. In addition to forming the general winning pattern (GWP), players must accumulate at least 8 points by matching at least one scoring pattern in order to declare a win. Among the 81 patterns, 56 are highly valued and are

810 referred to as major patterns, since most winning hands usually include at least one of them. Some
 811 special patterns do not adhere to the GWP, such as *Seven Pairs*, *Thirteen Orphans*, and *Knitted*
 812 *Straight*, as illustrated in Fig 5D.

813 The final scores of each player depend on the winner’s fan value and the provider of the 14th winning
 814 tile. Specifically, if the winner makes a winning hand of x fans by drawing a tile themselves, they
 815 receive $8 + x$ points from the other three players. Instead, if the 14th winning tile comes from
 816 another player, either discarded or added to the promoted pung, the winning player receives $8 + x$
 817 points from the provider of this tile, and only 8 points from the other two players.

819 B.2 MCR AS AN ENVIRONMENT

820 As an environment, MCR exhibits several unique characteristics that pose challenges to algorithms.

821 First, the 8-point-to-win rule of MCR adds an additional requirement to the hand patterns. This
 822 requirement excludes many hand patterns that would otherwise be valid GWPs. Agents must be
 823 capable of distinguishing between valid and invalid hand patterns to achieve a high level of
 824 performance. In addition, the various scoring patterns of MCR render the environment multi-goaled.
 825 Although most patterns comply with the GWPs, some special patterns do not. Notably, in many
 826 situations, these special patterns can be the closest and easiest goals to pursue. These special pat-
 827 terns add to the diverse choices of goals other than GWPs and thus require effective exploration by
 828 agents.

829 Besides, the state transitions of Mahjong can be approximately represented by a directed acyclic
 830 graph. To win a game, agents are expected to make around 10 to 40 consecutive decisions. Mis-
 831 takes or poorly sampled actions in Mahjong can lead to much worse game states and are hard to
 832 recover from, such as destroying some **melds**. Such a property of Mahjong conflicts with the need
 833 for exploration and poses additional challenges to learning-based agents. Furthermore, Mahjong
 834 involves high randomness and uncertainty from drawing tiles to opponent moves. During gameplay,
 835 newly encountered game states are rarely seen during training, and it is difficult and impractical to
 836 measure the similarity between states to draw on past experience. Thus, Mahjong predominantly
 837 presents out-of-distribution (OOD) states to its agents and imposes high demands on its agents’
 838 generalization capabilities.

840 B.3 REWARD SETTING FOR MCR MAHJONG ENVIRONMENT

841 In MCR Mahjong environment, we implement dense rewards to encourage agents to approach a
 842 winning hand more quickly, by incorporating **Shanten Distance** to calculate the reward in each
 843 step. **Shanten Distance** measures the minimum distance between the agents’ current hand and any
 844 valid winning pattern. Thus, agents receive a small positive reward by decreasing **Shanten Distance**
 845 and a small penalty by increasing **Shanten Distance**.

846 Additionally, MCR Mahjong environment differentiates between winning by self-drawing and win-
 847 ning with a tile from other players. Agents will receive higher rewards if they win by self-drawing,
 848 and other players will receive the same penalty for losing. Otherwise, it will receive a positive re-
 849 ward, but the player who played the last tile will receive a larger penalty to discourage reckless play.
 850 Table 7 presents the reward settings for MCR Mahjong Environment.

853 C EXPERIMENT SETUP AND CONFIGURATIONS

854 We conducted our experiments on Intel Xeon Gold 6348 CPU@2.6GHz platform with one Nvidia
 855 GeForce 3080 GPU and 1024GB RAM. For the software platform, we use Python 3.9.16, CUDA
 856 12.4, Pytorch 2.5.1, and PyMahjongGB 1.2.0 on Ubuntu 20.04.

857 Tables 8, 9, and 10 present the experimental configurations for the Blackjack, Maze, and MCR
 858 Mahjong environments, respectively. These configurations were determined via manual parameter
 859 searching and comparative analysis of results upon agent convergence. For the MPPO students in
 860 the MCR Mahjong environment, as they continue training from behavior-cloning checkpoints, their
 861 policy networks are frozen for the first 1000 GPU iterations to fit the value networks alone without
 862 breaking the policy.

864
865

866 Table 7: Reward Settings for MCR Environment

Agent Event	Value
Flat Step Penalty	-0.0006
Decrease in Shanten Distance	0.07
Increase in Shanten Distance	-0.07
Win by Self-drawing	0.8
Win with Other Player's tile	0.6
Game Lost	-0.2
Game Lost with playing the final tile	-0.5
Nobody Wins	0

867
868
869
870
871
872
873
874
875
876
877
878
879
880
881
882

883 Table 9: Maze Experiment Configuration

Entry	Setting	Entry	Setting
Replay Buffer	Iteration Per		
-Size	8200	-Model Sync	1
GAE Lambda	0.98	Entropy Coeff	0
Batch Size	8192	Entropy Decay	1
Policy Coeff	1	Value Coeff	0.5
Gamma	1	Learning Rate	5e-5
PPO Epoch	3	PPO Clip	0.05
Normal Actor	75	LfD Actor	5
Gail/Sail		Gail/Sail	
-Discriminator		-Learning Rate	1e-5
-Steps/Iteration	8	-Run Duration	1 hour

886
887
888
889
890
891
892
893
894
895

Table 8: BlackJack Experiment Configuration

Entry	Setting	Entry	Setting
Replay Buffer	Iteration Per		
-Size	4100	-Model Sync	1
GAE Lambda	0.98	Entropy Coeff	0
Batch Size	4096	Entropy Decay	1
Policy Coeff	1	Value Coeff	0.1
Gamma	1	Learning Rate	1e-2
PPO Epoch	3	PPO Clip	0.05
Normal Actor	76	LfD Actor	4
Gail/Sail		Gail/Sail	
-Discriminator		-Learning Rate	1e-5
-Steps/Iteration	8	Run Duration	1 hour

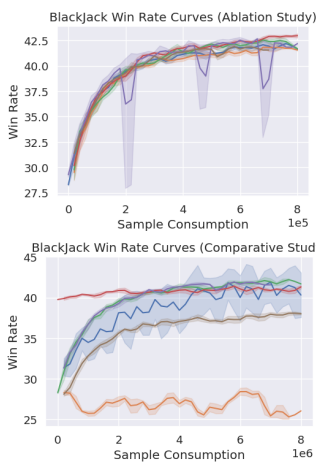
896

897

898

899

900



901

902

903

904

905

906

907

908

909

910

911

912

913

914

915

916

917

Table 10: MCR Mahjong Experiment Configuration

Entry	Setting	Entry	Setting
Replay Buffer	Iteration Per		
-Size	4100	-Model Sync	1
GAE Lambda	0.98	Entropy Coeff	1.5e-1
Batch Size	4096	Entropy Decay	0.99998
Policy Coeff	1	Value Coeff	1
Gamma	1	Learning Rate	1e-5
PPO Epoch	5	PPO Clip	0.05
Normal Actor	70	LfD Actor	10
Gail/Sail		Gail/Sail	
-Discriminator		-Learning Rate	1e-5
-Steps/Iteration	5	Run Duration	7 Days

Figure 6: Win Rate Curves During Training

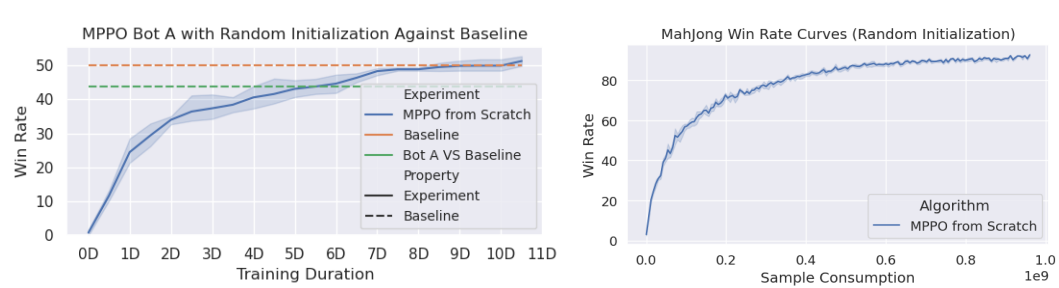
918 **D WIN RATE CURVES**
919920 Figure 6 presents the win rate curves for all experimental runs in the ablation study and comparative
921 study. For each environment, we use Bot A to generate demonstration trajectories, which
922 are utilized by all variants of MPPO in the ablation study and by all methods in the comparative
923 study, except for PPO. For experiments in Mahjong environment, all methods are initialized with
924 behavior-cloning checkpoints except DQfD, which has its own behavior-cloning pre-training phase
925 before reinforcement learning.926 It should be noted that the "win rate" metric presented in this section refers to the win rate of games
927 generated during training, which differs from the win rates reported in the experiment section of
928 the main text. During training, actors sample from action distributions of behavior policies, while
929 during testing, actors always take the action with the highest logit value. In our original experiments,
930 the sample generation rate and the sample consumption rate were recorded at fixed time intervals;
931 however, to compare the performance of different algorithms, these metrics have been converted to
932 accumulated sample consumption.934 **E USE OF LARGE LANGUAGE MODEL**
935936 In the preparation of this manuscript, the author utilized a large language model (LLM) for the
937 purpose of text polishing and refinement. This includes improving grammar, sentence structure, and
938 overall clarity. The author remains solely responsible for the entire academic content, including all
939 ideas, arguments, and conclusions presented herein.942 **F COMPARATIVE ANALYSIS OF STYLE DISTANCE METRICS**
943944 We re-calculate D_{policy} for BlackJack, Maze, and Mahjong environment using W_2 by setting
945 $d_A(a_i, a_j) = 1, \forall i \neq j$ and $d_A(a_i, a_i) = 0$. The Pearson correlation coefficient between these
946 two sets of aggregated distances was 0.9742, indicating a very strong positive correlation and con-
947 firming that TV divergence is a highly consistent relative measure for play style difference in our
948 contexts.949 To address the relationship between the Total Variation (TV) divergence and the 2-Wasserstein (W_2)
950 distance for measuring policy difference, we conducted a correlation analysis. We recomputed the
951 D_{policy} metric for the Blackjack, Maze, and Mahjong environments using the W_2 distance, defining
952 the ground metric on the discrete action space as $d_A(a_i, a_j) = 1, \forall i \neq j$. The per-state distances
953 were aggregated into a global $D_{policy}(W_2)$ following the same expectation as in Eq. equation 2.
954 The results are shown in Table 11, 12, and 13. The Pearson correlation coefficient between the
955 TV-based and the W_2 -based D_{policy} across all evaluated policy pairs was 0.9742. This near-perfect
956 positive correlation confirms that the TV divergence serves as a highly consistent and reliable relative
957 measure for play-style difference in our contexts, justifying its use for comparative analysis in this
958 work.960
961
962
963
964
965
966
967
968
969
970
971
Table 11: $D_{policy}(W_2)$ results for Maze
Agents Optimal Bot A Bot B
PPO .057±.003 .510±.005 .494±.004
MPPO A .084±.001 .469±.010 .536±.011
MPPO B .076±.004 .536±.011 .470±.013960
961
962
963
964
965
966
967
968
969
970
971
Table 12: $D_{policy}(W_2)$ results for Mahjong
Agents MPPO PPO
Bot A 0.297±.019 0.678±.022
Bot B 0.328±.006 0.691±.010
Bot C 0.279±.016 0.772±.022968
969
970
971
Table 13: $D_{policy}(W_2)$ results for BlackJack
Agents Optimal Policy Bot A
PPO 0.042±.009 0.259±.007
MPPO 0.135±.004 0.150±.011968
969
970
971
Table 14: Mahjong MPPO A Rand. Init. Results
Metric Warm Start Random Initialization
Win Rate 51.05±1.43 51.31±1.51
 D_{policy} 0.297±.016 0.305±.010

972 G MAHJONG MPPO AGENT WITH RANDOM INITIALIZATION
973

974 In the main experiments, MPPO and PPO agents in the Mahjong environment were warm-started
975 from behavior cloning (BC) checkpoints derived from their respective demonstrator bots. We clarify
976 that this warm-start is employed solely to reduce wall-clock time and resource consumption and is
977 not a methodological prerequisite for MPPO.

978 To validate this claim, we conducted an ablation study on the Mahjong environment using Bot A's
979 demonstration data. We compared an MPPO agent initialized from a BC checkpoint against an
980 MPPO agent initialized from random weights. All other experimental settings, including network
981 architecture, hyperparameters, and the mixture ratio of demonstration data ($\beta = 0.05$), remained
982 identical.

983 The results are summarized in Table 14. The final win rates were nearly identical, and the policy
984 distance to the demonstrator remained low in both cases. This confirms that the demonstration data
985 integrated via the MPPO objective is sufficient to effectively guide policy improvement and style
986 preservation, even without a pre-trained policy. The complete win rate curve against the baseline
987 bot and the corresponding training curve for this experiment are presented in Figure 7 and Figure 8,
988 respectively.



1000 Figure 7: Win Rate Against the Baseline for MPPO Agent A When Trained from Random Initialization. Figure 8: Win Rate Curves During Training
1001 for MPPO Agent A (Random Initialization).

